

**Interference effects in angular streaking with a rotating terahertz field**A. K. Kazansky,<sup>1,2,3</sup> A. V. Bozhevolnov,<sup>4</sup> I. P. Sazhina,<sup>5</sup> and N. M. Kabachnik<sup>3,5,6,\*</sup><sup>1</sup>*Departamento de Física de Materiales, UPV/EHU, E-20018 San Sebastian/Donostia, Spain*<sup>2</sup>*IKERBASQUE, Basque Foundation for Science, E-48011 Bilbao, Spain*<sup>3</sup>*Donostia International Physics Center (DIPC), E-20018 San Sebastian/Donostia, Spain*<sup>4</sup>*Sankt Petersburg State University, Universitetskaya nab. 7/9, Sankt Petersburg 199164, Russia*<sup>5</sup>*Skobeltsyn Institute of Nuclear Physics, Lomonosov Moscow State University, Moscow 119991, Russia*<sup>6</sup>*European XFEL GmbH, Albert-Einstein-Ring 19, 22761 Hamburg, Germany*

(Received 23 October 2015; published 11 January 2016)

A method of angular streaking with a rotating terahertz electric field for photoelectrons produced by femtosecond extreme ultraviolet pulses is suggested and theoretically analyzed. The method can be used for free electron laser (FEL) pulse characterization on a shot-to-shot basis. It is shown that in related measurements an interesting phenomenon appears: formation of very bright and sharp features in the angular resolved electron spectra measured in the plane perpendicular to the collinear beam direction. These features are similar to the conventional caustics in the wave propagation. The caustics are accompanied by a well-developed interference structure. The intensity distribution along the caustic is determined by the envelope of the FEL pulse.

DOI: [10.1103/PhysRevA.93.013407](https://doi.org/10.1103/PhysRevA.93.013407)**I. INTRODUCTION**

Streaking with an optical laser field is a well-established method in attosecond physics. First used in attosecond metrology [1] it was further applied to time-domain measuring the Auger lifetime [2] and to directly measuring the temporal evolution of the electric field of few-cycle optical pulses [3]. With this technique, the time delay between the photoemission from different atomic subshells [4] and the delay between the emission of photoelectrons from localized core states of a metal and from delocalized conduction band states [5] have been measured. In an attosecond streaking experiment the photoelectrons produced by subfemtosecond extreme ultraviolet (XUV) pulses are steered by a linearly polarized infrared laser field. The laser field determines the electron final kinetic energy which depends on the time of electron emission. Thus, the temporal structure of the ejected electron wave packet is mapped to the electron energy spectrum.

Recently a modification of this method, namely, attosecond angular streaking with an almost circularly polarized laser, was suggested [6,7] where the photoelectrons are deflected by the rotating laser field. Thus the instant of ionization is mapped to the final angle of the electron linear momentum vector in the polarization plane. This method, which was dubbed “attoclock,” was used for measuring the time of electron penetration through a potential barrier [8] as well as the time delay between emission of two electrons in strong-field double ionization of an atom [9].

With the advent of free electron lasers (FELs), the task has arisen to measure and monitor the duration and temporal structure of ultrashort (femtosecond) FEL pulses. It is especially important for FELs which rely on the stochastic process of self-amplified spontaneous emission. Here the pulses are produced without a well-defined temporal profile which even varies from shot to shot. For the so-called seeded FELs the problem of pulse shape is not so critical; however,

measurements of the pulse duration are necessary also for them. Among various methods for a shot-to-shot study of temporal properties of the FEL pulses, streaking with terahertz (THz) fields has been suggested and successfully implemented [10]. This is an extension of the streaking techniques of attosecond metrology to the femtosecond domain. In Ref. [10] a multicycle THz linearly polarized pulse produced by the same FEL-driving electron bunch in an additional dedicated undulator structure has been used for streaking. Later on [11] a single-cycle linearly polarized THz pulse produced by an independent optical laser was been used for full temporal characterization of FEL pulses. This latter method was applied for characterization of an all-optical synchronization system at FLASH in Hamburg [12]. In addition, streaking with the THz field was successfully applied in laboratory experiments for measuring the duration of electron wave packets produced by a high-harmonic XUV source [13].

Developing further the analogy with the attosecond streaking, in this work we discuss angular streaking of photoelectrons with a circularly polarized THz field. In contrast to the angular streaking experiments in Refs. [7–9], where one and the same IR pulse was used both for ionization and for streaking of electrons, we consider a two-color pump-probe type of experiment where the photoelectrons are produced by a femtosecond XUV pulse and streaked by the rotating THz field. This method can be an alternative to the usual energy streaking with a linearly polarized THz field. An advantage of angular streaking is that one does the streaking over a full cycle, whereas streaking with a linearly polarized field is effective during about a quarter of a cycle where the electric field changes approximately linearly with time [7]. This softens the requirement for jitter between the XUV and THz pulses. Besides, the absolute value of the rotating electric field is constant which simplifies an analysis of the streaking results.

Our calculations show that under certain conditions very bright features are formed in the double differential cross section (DDCS) for photoelectron emission. These features are similar to the well-known caustics in optics. We have found a noticeable interference effect in the region of caustics which

\*Corresponding author: [nkabach@gmail.com](mailto:nkabach@gmail.com)

can be studied experimentally and bears information on the details of the temporal properties of the ionizing pulses. From the intensity distribution on the caustic one can retrieve the shape of the FEL pulse.

## II. THEORY

We consider a process of photoionization of an atom by an ultrashort (femtosecond) XUV or soft x-ray pulse in a strong THz field synchronized with the ionizing pulse. For calculating the DDCS, a simple theoretical approach based on the strong-field approximation (SFA) [14] is used. A detailed description of the approach can be found in Ref. [15]. The XUV pulse is supposed to be linearly polarized while the collinear THz beam is circularly polarized. Such a case within the above approximation was considered in detail in Ref. [16] for longer XUV and optical pulses. We choose the coordinate system with the  $z$  axis along the beams and the  $x$  axis along the linear polarization of the XUV beam. For simplicity, we consider ionization of an  $s$  shell, for example in He atoms. Within the SFA, the amplitude of photoionization is presented in the following form:

$$\mathcal{A}_{\pm}(\vec{k}) \sim \pm \frac{i}{2} \int_{-\infty}^{\infty} dt d_{sp}(k_0) \bar{\mathcal{E}}_X(t) \times Y_{1,\pm 1}[\theta_0(t), \phi_0(t)] \exp[i\Phi(t)]. \quad (1)$$

Here  $d_{sp}(k_0)$  is the radial part of the dipole amplitude of the XUV photoionization from the bound  $s$  to the continuum  $p$  state with impulse  $k_0$  (we have assumed that  $d_{sp}(k_0)$  is practically constant in the considered energy interval and set it equal to unity), the upper (lower) sign corresponds to the right (left) circularly polarized XUV components,  $\bar{\mathcal{E}}_X(t)$  is the envelope of the XUV pulse, and  $\Phi(t)$  is related to the Volkov phase [17]:

$$\Phi(t) = - \int_t^{\infty} dt' \left( \frac{1}{2} [\vec{k} - \vec{A}_L(t')]^2 - E_p \right). \quad (2)$$

Here  $\vec{k}$  is an asymptotic value of the electron linear momentum (after interaction with the THz field),  $\vec{A}_L(t)$  is the vector potential of the THz field,  $\vec{A}_L(t) = \int_t^{\infty} dt' \vec{\mathcal{E}}_L(t')$ , and  $E_p = \omega_X - |E_b|$  is the kinetic energy of photoelectron without the THz field, with  $\omega_X$  being the XUV carrier frequency and  $E_b$  the electron binding energy. The components of the electric field of the rotating THz pulse are taken as

$$\mathcal{E}_{Lx}(t) = \bar{\mathcal{E}}_L(t) \cos(\omega_L t) \quad \mathcal{E}_{Ly}(t) = \bar{\mathcal{E}}_L(t) \sin(\omega_L t), \quad (3)$$

where  $\bar{\mathcal{E}}_L(t)$  and  $\omega_L$  are the envelope and the carrier frequency of the THz field, respectively. The angles  $\theta_0$  and  $\phi_0$  are the emission angles of the photoelectron before it enters into the THz field. They are connected with the detection angles  $\theta$  and  $\phi$  as follows:

$$k_0 \cos \theta_0 = k \cos \theta, \quad (4)$$

$$\exp[i\phi_0(t)] = \frac{[k_x - A_{Lx}(t)] + i[k_y - A_{Ly}(t)]}{[k_0^2(t) - k_z^2]^{1/2}}, \quad (5)$$

where

$$k_0^2(t) = [\vec{k} - \vec{A}_L(t)]^2, \quad (6)$$

and  $k_x$  ( $k_y$ ) and  $A_{Lx}(t)$  [ $A_{Ly}(t)$ ] are the  $x$  ( $y$ ) components of vectors  $\vec{k}$  and  $\vec{A}_L(t)$ , respectively.

In what follows we assume that the electron is emitted in the  $(x, y)$  plane perpendicular to the photon beams, i.e.,  $\theta_0 = \theta = \pi/2$ . In this case the photoionization amplitude for the XUV pulse, linearly polarized along the  $x$  axis, is given by Eq. (1) with substitution of the  $Y_{1,\pm 1}$  function with the expression  $\sqrt{3/2\pi} \cos[\phi_0(t)]$ .

## III. RESULTS AND DISCUSSION

The DDCS, which is proportional to the square of the amplitude, has been calculated numerically for a Gaussian XUV pulse of varied duration and a three-cycle THz pulse with a frequency of 5 THz and a field strength of 300 kV/cm. The electric fields of the THz and XUV pulses used in this work are shown in Fig. 1(a) in arbitrary units. Only one-half of the THz pulse with the total duration of 600 fs is shown. In Fig. 1(b), the DDCS (color-scaled in arbitrary units) is shown as a function of the electron energy and the azimuthal emission

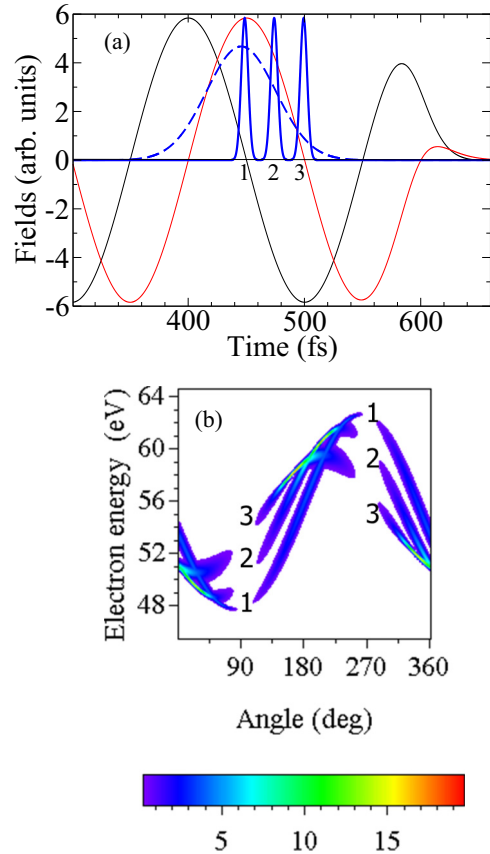


FIG. 1. (a) The electric fields of the second part of the THz pulse and the XUV pulses used in the calculations, in arbitrary units. Time is counted from the onset of the THz pulse. Thin black curve:  $\mathcal{E}_{Lx}$ . Thin red (light gray) curve:  $\mathcal{E}_{Ly}$ . Thick solid curves: XUV pulses (10 fs) at different time delays. Dashed curve: XUV pulse of 50 fs. (b) Color-scaled streaking spectra as a function of the emission angle of photoelectrons produced by three independent XUV pulses at different delays. Numbers correspond to the delays indicated in panel (a). For other parameters, see text.

angle  $\phi$  for the case when the XUV pulse is 10 fs [full width at half maximum (FWHM)] in duration, i.e., much shorter than the period of the THz pulse (200 fs). The three short pulses, shown in Fig. 1(a), correspond to the three relative positions of the XUV and THz pulses (different time-delays). Pulse 1 is set at the maximum of the  $x$  component of the THz vector potential. The corresponding angular distribution [curve 1 in Fig. 1(b)] has a cosine shape, with the intensity distribution along the line proportional to  $\cos^2 \phi$  with zero intensity at  $90^\circ$  and  $270^\circ$ . Spectra 2 and 3 correspond to the pulses 2 and 3 with different time-delays. One can see that the angular position of the maximum (minimum) electron energy and the intensity distribution depend on the delay, while the intensity zeros, defined by the zeros in the emission probability, remain at the same angles. Also the width of the spectra varies with the delay in the same way as it was established for linear streaking [1].

The behavior of the DDCS illustrated in Fig. 1(b) can be easily explained using a stationary phase (saddle point) approximation for calculating the integral in Eq. (1). This is a standard approach in the SFA (see, for example, Ref. [18]) and links this approach with the classical treatment. Indeed, the stationary phase points  $t_{st}$  are determined by the equation

$$\Phi'(t_{st}) = \frac{1}{2}[\vec{k} - \vec{A}_L(t_{st})]^2 - E_p = 0, \quad (7)$$

which corresponds to the classical relation between the final linear momentum and the time of electron emission. In the kinematics considered, Eq. (7) can be presented as

$$-kA_L(t_{st}) \cos[\phi - \phi_A(t_{st})] + A_L^2(t_{st})/2 = E_p - k^2/2, \quad (8)$$

where  $\phi_A(t_{st})$  is the azimuthal angle of the vector potential in the polarization plane at the moment  $t_{st}$ . For a given value of  $t_{st}$ , Eq. (8) defines the line  $k(\phi)$ . In what follows we call these lines *isochrones*. In each period of the THz field, Eq. (8) can have two, one, or no real solutions, depending on the value of  $t_{st}$ . Below, a special case is important, when the two solutions merge. We note that integration in Eq. (1) is limited by the time interval, when the XUV pulse is operative. If the pulse is very short, only one stationary point  $t_{st}$  contributes, and the angular streaking pattern has a simple cosine shape (see Fig. 1) described by Eq. (8) with a width determined by the duration of the FEL pulse.

When the temporal width of the XUV pulse increases, being still smaller than the period of the THz field, all  $t_{st}$ 's covered by the pulse contribute. The streaking pattern becomes wide and an interesting phenomenon appears: the formation of very bright sharp features near the edge of the streaking spectrum. A hint for their formation could be already seen in Fig. 1(b) in the area where the three lines intersect. Additionally, the interference effect (see below) increases the intensity of the bright features. This phenomenon is illustrated by Fig. 2(a) where the calculated DDCS is shown for the XUV pulse duration of 50 fs (FWHM). All other parameters are the same as those in Fig. 1. The DDCS is shown in logarithmic scale in false-color representation. The details of the streaking spectrum can be interpreted with the corresponding picture of classical isochrones, shown in Fig. 2(b). Note that the isochrones are calculated for the values of  $t_{st}$  covered by the XUV pulse. Comparing the two panels of Fig. 2, one sees that the DDCS is large in the "triangle" region where two

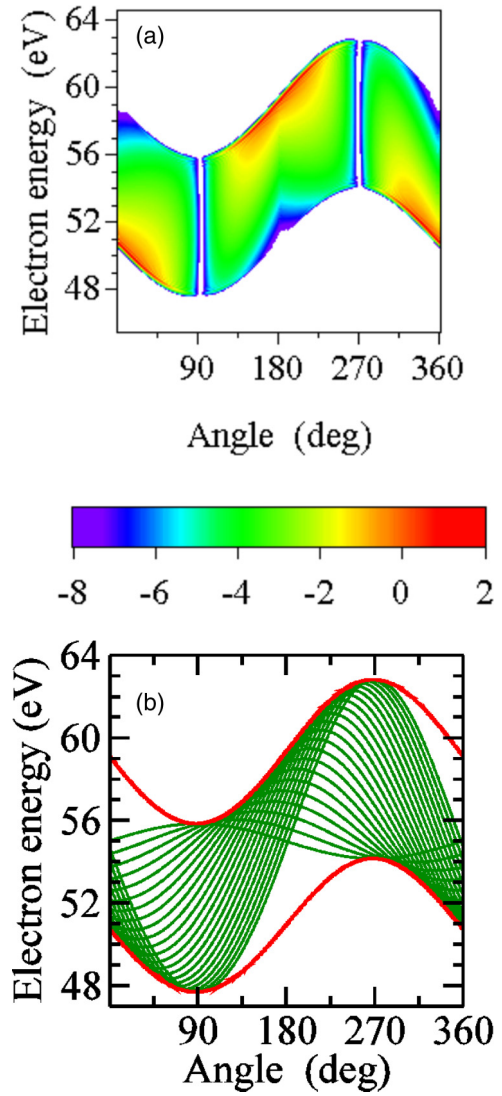


FIG. 2. (a) Color-scaled DDCS (in logarithmic scale) calculated for photoionization by a 50-fs XUV pulse in the THz field as a function of electron energy and emission angle. For other parameters, see text. (b) The isochrones (thin lines) for a set of  $t_{st}$  covered by the XUV pulse. Thick lines show envelopes (caustics).

isochrones pass through any point  $(\phi, k)$ . On the contrary, in the region where there are no passing isochrones, a cavity is formed. Very sharp bright features appear at the envelope of the set of the isochrones. These features are fully similar to conventional caustics in problems of wave propagation. Indeed, at the vicinity of each stationary phase point, the phase in Eq. (1) can be expressed as

$$\Phi(t) = \Phi(t_{st}) + \frac{(t - t_{st})^2}{2} \Phi_2(t_{st}), \quad (9)$$

where

$$\begin{aligned} \Phi_2(t_{st}) = \Phi''(t_{st}) = & -kA'_L(t_{st}) \cos[\phi - \phi_A(t_{st})] \\ & - kA_L(t_{st}) \phi'_A(t_{st}) \sin[\phi - \phi_A(t_{st})] \\ & + [A_L^2(t_{st})]' / 2. \end{aligned} \quad (10)$$

Then, the integral in Eq. (1) can be evaluated with the stationary phase method. The result reads

$$A_0(k, \phi) \cong -i\sqrt{3}d_{sp}(k_0)\bar{\mathcal{E}}_X(t_{st})\cos[\phi_0(t_{st})] \times \exp[i(\Phi(t_{st}) + \pi/4)] \frac{\sqrt{\pi}}{\sqrt{\Phi_2(t_{st})}}. \quad (11)$$

From this expression, it is clear that the DDCS sharply increases in a region where  $\Phi_2(t_{st})$  becomes small, forming the bright line along the caustic. At the caustic, the two solutions of Eq. (8) merge and with further increase of module  $|E_p - k^2/2|$  become complex. The caustics are determined by Eq. (8) and  $\Phi_2(t_{st}) = 0$ , where  $\Phi_2$  is given by Eq. (10). This set of equations is a parametric representation of the caustic with  $t_{st}$  as a parameter. With varying  $t_{st}$  inside the exciting XUV pulse, one can plot these lines as functions of the final electron energy and the azimuthal angle  $\phi$  of the electron emission. The caustics are shown in Fig. 2 by thick solid curves. Note that in this figure the isochrones are presented only for the values of  $t_{st}$  inside the FEL pulse, while the caustics are plotted without this limitation.

In the vicinity of the caustics, there is a region where two isochrones pass through any given point  $(\phi, k)$ . Within the quantum-mechanical picture, electrons emitted at the same angle with the same energy, but at different times, interfere. The contributions from the corresponding stationary points sum up coherently and this produces the interference pattern. The latter is shown in Fig. 3(a) which presents a part of the spectrum from Fig. 2(a) on a larger scale. In

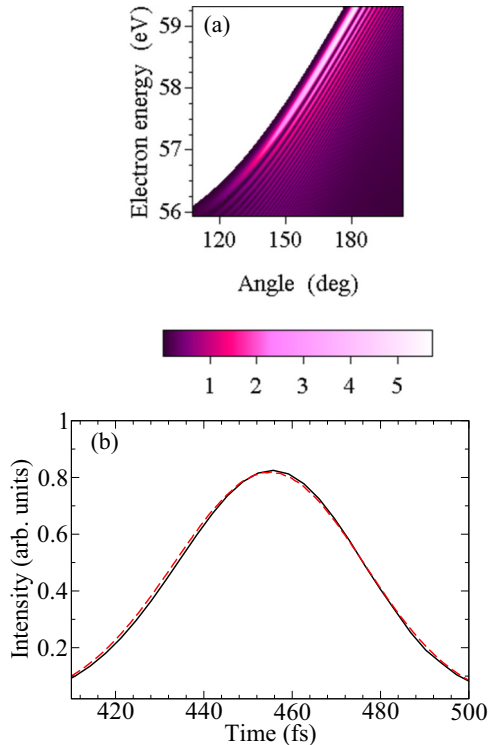


FIG. 3. (a) A part of the spectrum presented in Fig. 2(a) shown on a larger scale. An interference pattern in the DDCS is clearly seen in the vicinity of the caustic. (b) Comparison of the intensity profile of the original XUV pulse (black solid curve) and of the intensity distribution along the caustic (red dashed curve).

this particular example the energy interval between the first and the second maxima is about 0.2 eV. Using a standard semiclassical technique, one can show that the behavior of the DDCS in the vicinity of caustics can be described in terms of the conventional Airy function. A detailed derivation of this expression will be published elsewhere. Here we only note that asymptotically the Airy function can be presented as a cosine function with the phase proportional to  $kA_L/\omega_L$ . This relation reflects the scaling properties of the interference effect.

Since each point on the caustics corresponds to a well-defined emission time, the DDCS at these lines is directly related to the dependence of the envelope of the XUV pulse  $\bar{\mathcal{E}}_X(t)$  on the time. In Fig. 3(b) we show the envelope of the XUV pulse intensity (solid black line) used in the calculations. The dashed red line shows the pulse reconstructed using the intensity distribution along the caustic from Fig. 2(a) (divided by  $\cos^2 \phi$ ). The relation between angle  $\phi$  and  $t_{st}$  at the caustic follows from Eqs. (8) and (10). The shape of the reconstructed pulse perfectly coincides with the original XUV pulse.

Additionally, the existence of the interference pattern can be used for investigating small variations in the phase of the XUV pulse. Indeed, the electric field in the FEL pulse is  $\mathcal{E}_X = \bar{\mathcal{E}}_X(t) \cos[\omega_X t + \delta_X(t)]$ . The basic Eq. (1) is obtained within the rotating-wave approximation assuming that the phase of the XUV field  $\delta_X(t) = 0$ . However, in reality the pulse always contains some contaminating variations of its phase even for the seeded FEL. From the mechanism of the interference formation, described above, one can infer that the small phase variations  $\delta_X(t)$  should lead to corrugation of the interference pattern and thus could be registered within a single-shot regime. A detailed analysis of the phase variation and its influence on the interference pattern is beyond the scope of this paper.

It is worthy to note that the described interference effect becomes noticeable when the duration of the FEL pulse is comparable with the half-period of the THz field. Thus, in order to observe this effect for shorter FEL pulses one should increase the frequency of the THz field up to the far-infrared range (which is presumably feasible with modern experimental facilities [19]). In another extreme case when the XUV pulse is longer than the period of the THz field the DDCS pattern turns into the conventional picture of the sidebands which we considered early [16].

#### IV. CONCLUSIONS

In conclusion, we have suggested and discussed an interesting type of possible two-color streaking experiment, with a femtosecond linearly polarized FEL pulse accompanied by a circularly polarized THz pulse. In such an experiment, within a shot-to-shot regime, the photoionization DDCS observed in the plane perpendicular to the collinear photon beams may reveal very sharp and bright features. These features appear at the envelope of contributions from electrons ejected at different times of the FEL pulse. We have revealed similarity between these bright features in DDCSs and caustics in a wave propagation theory. It is shown that the caustics are accompanied by a well-developed interference structure. The intensity distribution along the caustics is related to the envelope of the XUV pulse and can be used for measuring its temporal variation on a shot-to-shot basis.

## ACKNOWLEDGMENTS

The authors acknowledge useful discussions with M. Meyer, T. Mazza, and M. Drescher. N.M.K. acknowledges hospitality and financial support from DIPC (Donostia/San

Sebastian) and from the theory group in cooperation with the SQS work package of European XFEL (Hamburg). A.V.B. acknowledges the support of St. Petersburg State University (Grant No.11.38.654.2013).

- 
- [1] M. Hentschel, R. Kienberger, Ch. Spielmann, G. A. Reider, N. Milosevic, T. Brabec, P. Corkum, U. Heinzmann, M. Drescher, and F. Krausz, *Nature (London)* **414**, 509 (2001).
- [2] M. Drescher, M. Hentschel, R. Kienberger, M. Uiberacker, V. Yakovlev, A. Scrinzi, Th. Westerwalbesloh, U. Kleineberg, U. Heinzmann, and F. Krausz, *Nature (London)* **419**, 803 (2002).
- [3] E. Goulielmakis *et al.*, *Science* **305**, 1267 (2004).
- [4] M. Schultze *et al.*, *Science* **328**, 1658 (2010).
- [5] A. L. Cavalieri *et al.*, *Nature (London)* **449**, 1029 (2007).
- [6] P. Dietrich, F. Krausz, and P. B. Corkum, *Opt. Lett.* **25**, 16 (2000).
- [7] P. Eckle, M. Smolarski, P. Schlup, J. Biegert, A. Staudte, M. Schöffler, H. G. Muller, R. Dörner, and U. Keller, *Nat. Phys.* **4**, 565 (2008).
- [8] P. Eckle, A. N. Pfeiffer, C. Cirelly, A. Staudte, R. Dörner, H. G. Muller, M. Büttiker, and U. Keller, *Science* **322**, 1525 (2008).
- [9] A. N. Pfeiffer, C. Cirelly, M. Smolarski, R. Dörner, and U. Keller, *Nat. Phys.* **7**, 428 (2011).
- [10] U. Fröhling *et al.*, *Nat. Photonics* **3**, 523 (2009).
- [11] I. Grguras *et al.*, *Nat. Photonics* **6**, 852 (2012).
- [12] S. Schulz *et al.*, *Nat. Commun.* **6**, 5938 (2015).
- [13] B. Schütte, U. Fröhling, M. Wieland, A. Azima, and M. Drescher, *Opt. Express* **19**, 18833 (2011).
- [14] L. V. Keldysh, *Sov. Phys. JETP* **20**, 1307 (1965).
- [15] A. K. Kazansky, I. P. Sazhina, and N. M. Kabachnik, *Phys. Rev. A* **82**, 033420 (2010).
- [16] A. K. Kazansky, A. V. Grigorieva, and N. M. Kabachnik, *Phys. Rev. A* **85**, 053409 (2012).
- [17] D. M. Wolkow, *Z. Phys.* **94**, 250 (1935).
- [18] J. Itatani, F. Quere, G. L. Yudin, M. Yu. Ivanov, F. Krausz, and P. B. Corkum, *Phys. Rev. Lett.* **88**, 173903 (2002).
- [19] N. Stojanovic and M. Drescher, *J. Phys. B* **46**, 192001 (2013).